Available online at www.sciencedirect.com

SciVerse ScienceDirect

journal homepage: www.elsevier.com/locate/he

Carbon xerogels as electrochemical supercapacitors. Relation between impedance physicochemical parameters and electrochemical behaviour

P.S. Fernández [a,*], A. Arenillas [b], E.G. Calvo [b], J.A. Menéndez [b], M.E. Martins [a]

[a] Instituto de Investigaciones Fisicoquímicas Teóricas y Aplicadas (INIFTA), Facultad de Ciencias Exactas, UNLP, CCT La Plata-CONICET, Boulevard 113 y 64, 1900 La Plata, Argentina

[b] Instituto Nacional del Carbón, CSIC, Apartado 73, 33080 Oviedo, España, Spain

ARTICLE INFO

Article history:
Received 25 August 2011
Received in revised form
22 December 2011
Accepted 31 January 2012
Available online 25 February 2012

Keywords:
Electrochemical supercapacitors
Porous electrodes
Electrochemical impedance spectroscopy
Interfacial area

ABSTRACT

The electrochemical behavior of carbon xerogels was studied with the aim of analyzing the performance of the materials used as electrochemical supercapacitors (SC) and to relate with physicochemical parameters. These materials have areas involving 1500–2000 m^2/g measured with the BET equation and a range of pore size distributions.

Conventional electrochemical techniques were used as cyclic voltammetry (CV), which allowed electrochemical characterization of different materials, and chronopotentiometry (CD), in order to determine the charge storage capacity of the xerogel at different currents or discharge rates.

Experimental results using electrochemical impedance spectroscopy (EIS) were interpreted with a physicochemical model that permitted identifying different parameters of the electrode, which explain the differences in the behavior of materials.

1. Introduction

The electrochemical supercapacitors (SC) are devices through which electric charges are stored in the electrical double layer (EDL) for each of the high surface area carbon porous electrodes involved. On the other hand, in the batteries, the charge storage process is essentially faradaic, since electron transfer takes place that changes the chemistry of electroactive compounds. The differences in the processes that occur in each of these devices generate features that are opposed, making them suitable for use in different technologies or working in a complementary manner in a single system [1]. The most striking differences between them are: i) The SC can store a much smaller amount of energy than the batteries (~10 $Whkg^{-1}$ for SC in aqueous electrolyte and 150–250 $Whkg^{-1}$ for a lithium-ion battery). ii) The power densities of the SC are even nine times higher than those of lithium-ion batteries, namely, 6.4 vs. 0.7 $kWkg^{-1}$ [2,3]. iii) A device based on charge and discharge of the EDL involves an entirely reversible process allowing a number of charge–discharge cycles of several orders of magnitude higher than batteries, in which cycle to cycle are produced changes that gradually degrade electrodes irreversibly [1].

In this work, we have synthesized and chemically activated carbon xerogels with high area and a range of pore size distribution. This allowed evaluating the behavior of each

* *Corresponding author*. Tel.: +54 221 425 7430; fax: +54 221 425 4642.
E-mail addresses: pablosf23@yahoo.com.ar (P.S. Fernández), aapuente@incar.csic.es (A. Arenillas), mariaelisamartins@gmail.com, mmartins@inifta.unlp.edu.ar (M.E. Martins).

0360-3199/$ – see front matter
doi:10.1016/j.ijhydene.2012.01.154

material as SC and their relationship with physicochemical properties of the carbons. Carbon gels are porous materials interesting for use in this area due to its structural characteristics that can be selected by adjusting the conditions used in the synthesis and subsequent processing of materials [4–6].

While this work can be framed within a specific application, it focuses on discussing basic aspects of electrochemistry that are often neglected, incurring in wrong definitions or assigning a determined behavior to erroneous factors. In this context, there is a very detailed discussion about electrochemical interface area, which is important parameters for all basic electrochemistry areas, especially for electroanalytical chemistry and electrocatalysis discussions.

2. Experimental

Carbon xerogels were used, which were impregnated with PTFE TE-3893® (an aqueous dispersion of a fluoropolymer resin): i) M1 10% PTFE; ii) M2 30% PTFE; iii) M3 15% PTFE; iv) M4 10% PTFE. Moreover, as comparative parameter was used carbon Supra 30 DLC (Norit®) 10% PTFE, designated S30. In all cases a minimum quantity of PTFE were used in order to bring about a minimum change on the properties of the as-prepared carbon material.

The electrodes were prepared by introducing those carbon xerogels impregnated with resin inside a steel pillbox in which had previously placed a Ni wire skeleton, then applying a pressure of 2100 $kgcm^{-2}$.

2.1. Synthesis of carbon Xerogeles

Carbon xerogels used in this work were constructed as follows. First, an organic xerogel (OX) was synthesized using an RF solution through a microwave radiation treatment, according to a procedure described elsewhere [7]. Subsequently, several materials were obtained: i) M1 is an OX prepared with an RF solution (pH = 6.5) and activated with KOH in a microwave oven ($T = 700\ ^{\circ}C$ for $t = 6$ min). ii) M2 was synthesized in the same way as for M1, being activated in a horizontal furnace during 2 h iii) M3 is an OX prepared with an RF solution (pH = 5.8). Then, it was stabilized heating at 800 °C in N_2 atmosphere to obtain a carbon xerogel, which was then activated with KOH in the same way as that for M2. iv) M4 was obtained equally to M3 but RF solution with pH = 6.5.

2.2. Electrochemical system

The electrochemical experiments were performed using a cell of three electrodes in 6M KOH aqueous solution. As working electrode teflonated carbon xerogels were used; the counter electrode was a nickel mesh and as the reference electrode was used Hg/HgO/6M KOH (+0.098 vs. NHE). In the text, the potentials are referred to the electrode employed as reference. All experiments were performed at room temperature.

2.3. Characterization

The textural characterization of the samples was carried out through physical adsorption of N_2 at 77K, using a Micromeritics model TriStar II. The volume of micropores, V_{mic} (cm^3g^{-1}), was achieved by applying the Dubinin-Radushkevich (DR) method [8] to the N_2 adsorption isotherms. From the volume of the micropores and the average size of the pores (L_p) can be obtained the surface area of micropores ($S_{mic} = 2V_{mic}/L_p$) applying Stoeckli equation [9]. The BET area was also evaluated using the N_2 adsorption isotherms [10]. The structure of the samples was assessed using a transmission electron microscope (TEM). The images were taken with a JEOL JEM-2000 EX II.

The conductivity measurements of carbons were carried out at atmospheric pressure, using an apparatus made in the laboratory, which is a modification of the van der Pauw technique [11].

3. Results and discussion

3.1. Carbon characterization

3.1.1. Transmission electron microscopy (TEM)

Fig. 1A and B show images of one of the xerogels with and without Teflon, respectively. Fig. 1A clearly exhibits the structure of a typical amorphous xerogel, whereas the 1B shows the loss of the porous structure characteristic of the material due to masking by the homogeneous deposition of polymer on the surface.

3.1.2. Textural characterization

Fig. 2 shows the isotherms performed with N_2 at 77K for different electrodes. Usually, measurements are made with the carbons in his pristine state. Although we found that the addition of 10% PTFE slightly changes the features of those isotherms, the fact that for the construction of the electrodes is required to apply pressure to the carbons impregnated with Teflon leads to a decrease of the textural characteristics of the materials. For this reason, it was necessary to obtain the isotherms of the electrode materials. These were classified into two groups. Thus, M2 and S30 samples exhibit a type I isotherm, which correspond to the presence of predominantly microporous materials (but also have small mesopores), while M1, M3 and M4 reveal hysteresis cycles, showing isotherms of type I-IV, being characteristic of micro-mesoporous materials [12].

Table 1 shows a summary of the parameters calculated by means of the isotherm measurements, which are related to the porosity and surface area of materials. These are: i) the area calculated by BET equation (S_{BET} in m^2g^{-1}); ii) the volumes represented by mesopores and micropores in cm^3g^{-1}; iii) the average size of micropores, L_P in nm. Moreover, in the last column is placed the solid conductivity measurement, σ, expressed in Scm^{-1}.

3.2. Electrochemical measurements

3.2.1. Cyclic voltammetry (CV) and potentiometry (CD charge and discharge)

VC was conducted by performing triangular potential sweeps at $v = 1.10^{-3}$, 3.10^{-3}, 5.10^{-3} and 1.10^{-2} V^{-1}. Potential limits were set to show only the region of purely capacitive behavior.

Fig. 3 shows voltammograms for all the carbons utilized, made at $v = 1.10^{-2}$ V^{-1}. For these electrodes a clear deviation

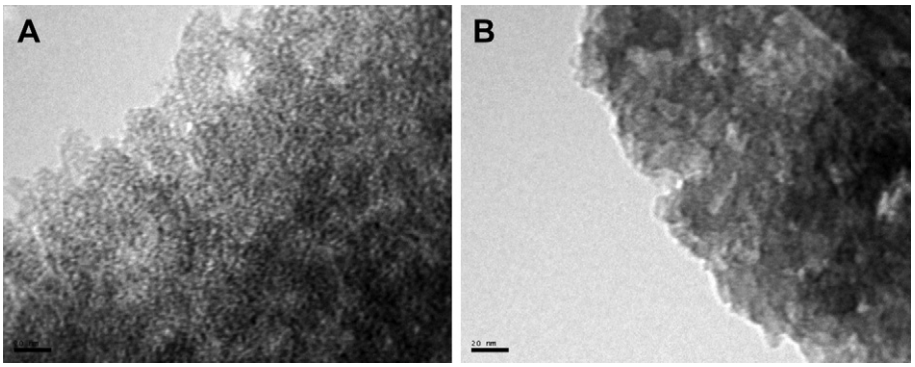

Fig. 1 – TEM images of a xerogel without (A) and with Teflon (B).

from ideal behavior can be observed, since they do not exhibit the typical rectangular shape that is observed for a pure capacitor. Nevertheless, an important part of this deviation is due to the intrinsic resistance of the system employed to evaluate the materials. This fact causes that the parameters measured in these experiments can not be directly compared with those obtained with materials using another system or in a capacitor. Therefore, in order to have a direct parameter for comparison it was purchased commercial coal S30, which is used in the manufacture of SC. While all voltammograms show significant resistive components, in the figure stand out clearly the xerogel M2, which, by reversing the potential sweep in the positive direction reaches the maximum positive current faster. In addition, throughout the entire potential window displays the higher absolute current values being directly related to the charge of the electric double layer. Similarly, electrodes constructed with materials identified S30 and M4 performed better than those made with M1 and M3.

The CDs were carried out between −0.20 and −0.90 V. The electrodes were charged at 88.6 mAg^{-1} and subsequently discharged at different currents.

The potential-time curves demonstrate small deviations from linearity due to the occurrence of charge transfer reactions. Moreover, the variation of capacities with different discharge rates gives an idea of the internal resistance of the system. Because the only change made between measurements is the composition of ET, it is valid to assign the dissimilarities to the different resistive components introduced by the carbons. These are: i) the electronic conductivity of the solid, σ (Table 1) and ii) the effective conductivity of the electrolyte, i.e., the conductivity of aqueous electrolyte within the porous electrode matrix (k).

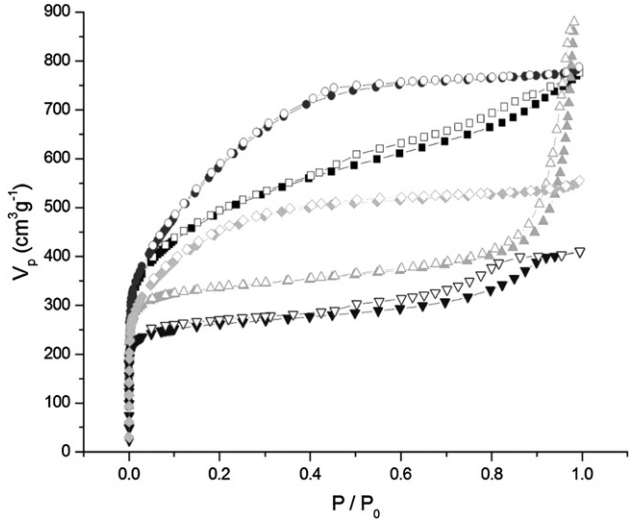

Fig. 2 – Isotherms for M1(■), M2(●), M3(▲), M4(▼), S30(▯).

Fig. 4 exhibits the dependence of C with the discharge rate. At low currents, all carbons show higher C than the commercial product S30. Under these circumstances, where the resistances of the system have a secondary role, are prominent those materials with higher specific areas and therefore, as when working with relatively similar materials, exhibit higher interfacial area obtained through BET model. Nevertheless this behavior is not always the same, because the area measured through isotherms depends on access of N_2 to the pores, while for the formation of the EDL is the electrolyte that must be able to join them. It is well known that in experimental conditions N_2 is able to access pores smaller than water molecules [13].

Thus, capacities obtained at low currents are indicative of the interfacial area of the electrode. The fact that M1 (S_{BET}: 1786) has a C markedly higher than that of M2 (S_{BET}: 2089) indicates that the pore distribution of M1 generates greater access of the electrolyte to the porous matrix of this electrode, probably due to the presence of a greater amount of large mesopores and even macropores (the V_{ads} increases even at high pressures). Correspondingly, one can conclude that the aqueous electrolyte is in direct contact with a lesser electrode surface in electrode constructed with S30 than with those

Table 1 – Textural characteristics of the carbons studied, obtained by the N_2 adsorption isotherms at 77K, and conductivity values of the electrodes (active material and binder used).

Muestra	S_{BET}	V_{meso}	V_{micro}	L_p	$\sigma.10^2$
M1	1786	0.54	0.65	1.8	0.42
M2	2089	0.54	0.67	1.8	0.66
M3	1316	0.83	0.52	1.2	0.08
M4	1020	0.23	0.40	1.0	0.09
S30	1664	0.31	0.54	1.6	0.12

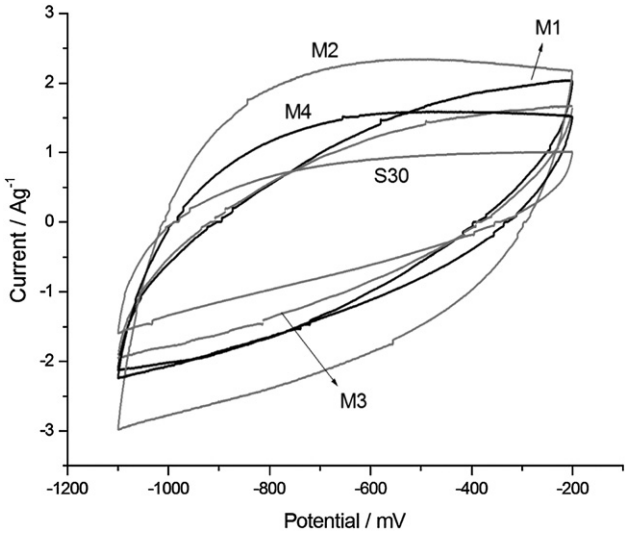

Fig. 3 – Voltammograms performed at $v = 1.10^{-2}\ V^{-1}$ for all the materials employed.

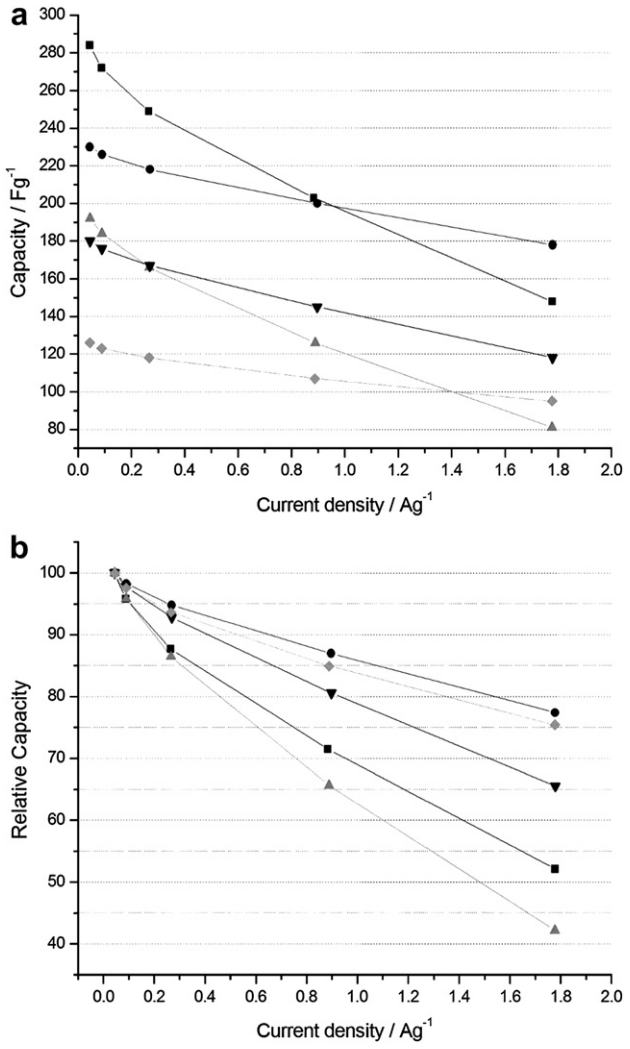

Fig. 4 – Capacity (a); relative capacity (b). M1(■), M2(●), M3(▲), M4(▼), S30(●).

electrodes containing M3 and M4, isotherms shedding a similar conclusion as above. We shall see later through EIS measurements, that one can indirectly measure the accessibility of the electrolyte into the pores of the xerogels.

As the current increases it can be seen a drop in C for all materials, being higher for M1 and M3. In this regard, both M2 and M4 xerogels as carbon S30 are showing the best results, which agree very well with that observed in the VC experiments. Taking into account the values of C at high currents, it can be observed that all the xerogels, excepting M3, outperform S30, being the storage capacity of charge of M2 higher than that of S30 in more than 80 Fg^{-1}.

3.2.2. *Electrochemical impedance spectroscopy (EIS)*

EIS measurements were carried out at −0.3 V by imposing a sinusoidal perturbation of 15 mV in the 0.5 mHz ≤ *f* ≤ 50 kHz frequency range. The potential of −0.3 V was chosen with the aim of minimize the pseudocapacitance contribution to the electric double layer in the electrodes. This approach makes it possible to devise a simple electrochemical impedance model with the purpose of derive the impedance function of the system, and draw direct conclusions from the fitting procedure. This topic is discussed in more detail in the next section.

The typical response of a porous electrode is shown in Fig. 5. At the highest frequencies, a semicircle can be seen. This capacitive contribution has been related to poor electrical contact between the solid particles and with the current collector (occurs because of the contact between the carbon particles and between carbon particles and the current collector) [14].

In the range of high-medium frequencies, the spectra clearly show a linear behavior with a slope of approximately 45°, and below a characteristic frequency, the value of the angle increases to almost 90°. This type of response is associated with the distribution of potential, due to finite conductivities of the electrolyte and solid phases, within the porous structure [15].

3.2.2.1. *Theoretical analysis - physicochemical model.* A theoretical analysis of the dynamic electrochemical response of

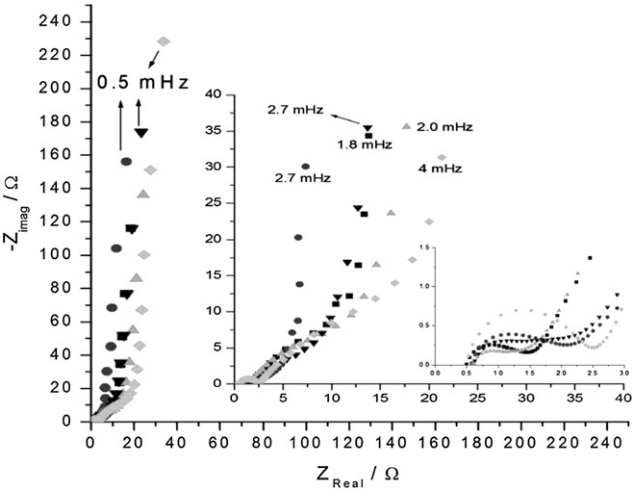

Fig. 5 – Nyquist diagrams. M1(■), M2(●), M3(▲), M4(▼), S30(●). Insert (a) corresponds to behavior at low frequencies and (b) At medium frequencies.

the system is presented and a physicochemical model is derived. In order to identify the structural and kinetic parameters of the different electrodes studied, the impedance function resulting from the model was fitted to the experimental EIS data.

The electrode is modeled as an isotropic porous structure, whose voids are filled with electrolyte. The model, based on the classic theory of porous flooded electrodes [16,17], takes into account the porous nature of the material, the solid and liquid conductivities and the electrochemical processes at the solid material/electrolyte interface.

Fernández et al. carefully explain the development of this model in a previous work [14]. The final expression for the total impedance Z_p may be expressed as:

$$Z_p = \frac{L}{A_p(\kappa+\sigma)}\left[1+\frac{2+\left(\frac{\sigma}{\kappa}+\frac{\kappa}{\sigma}\right)\cosh\nu}{\nu\sinh\nu}\right] \quad (1)$$

where ν is given by:

$$\nu = L\left(\frac{\kappa+\sigma}{\kappa\sigma}\right)^{1/2} Z_i^{-1/2} \quad (2)$$

Z_i is the interfacial impedance per unit volume, A_p is the transverse electrode geometric area and L is the electrode thickness. The conductivities previously defined have units of $\Omega^{-1}cm^{-1}$.

3.2.2.2. Interfacial impedance (Z_i). In order to calculate the total impedance Z_p using (1), an expression for Z_i (Ωcm^3) is required. In our case, the interfacial impedance only implies the double layer capacitance impedance (Z_{dl}),

$$Z_i = Z_{dl} \quad (3)$$

where

$$Z_{dl} = \frac{1}{j\omega C_{dl}} \quad (4)$$

C_{dl} is the double layer capacitance per unit volume (Fcm^{-3}); j is the imaginary number; and $\omega = 2\pi f$ (f, frequency of the perturbing signal).

It should be pointed out that our system has two capacitances linked in parallel, namely, the double layer capacitance and the pseudofaradaic capacitance. The latter was neglected in this model because EIS measurements were conducted at a potential value where the contribution of this capacitance to the total electrode capacity was very low.

3.2.2.3. Fitting procedure. With the aim of identify the parameters of the system, a fitting procedure of the experimental impedance data in terms of the theoretical impedance function, Z_p, was accomplished. A fitting program was developed, based on the Nelder-Meade simplex search algorithm [18,19]. The fitting was considered acceptable when J_p, the cost function, is $J_p < 5.10^{-3}$.

$$J_p = \frac{1}{K}\sum_k \left|\frac{Z_e(\omega_k) - Z_p(p,\omega_k)}{Z_e(\omega_k)}\right|^2 \quad (5)$$

where K is the number of frequencies employed in the experiments, and Z_e and Z_p correspond to experimental and theoretical data, respectively, corresponding to the frequency ω_k.

As contact between particles is not considered, the higher frequency values were neglected from the fitting procedure.

A comparison of the experimental results and the theoretical diagrams derived from the fitting procedure for all the electrodes evidences a good fit. Experimental and theoretical, Nyquist and Bode diagrams for M2 electrode are shown in Fig. 6.

3.2.2.4. Calculation and analysis of electrochemical parameters. It must be emphasized that S_{EIE}, the interfacial area per unit gram, is a parameter derived after fitting the experimental results and from the electrochemical point of view, it is a measure of the real area that takes part in the electrode reaction. This is a point of extreme importance because the data provided by the BET method for specific area give information about the whole material used in the experiment, while the interfacial area identified from the EIS analysis, is real information about the fraction of material that actually participates in the electrode/solution interfacial process.

The capacity of the electric double layer per electrode unit volume (C_{dl}) is obtained from the fitting procedure for each electrode. This parameter can be related to the values of C, obtained from CD measurements, when multiplied by the volume of each of the electrodes (LA_p). Thus, Table 2 shows the values of capacity obtained by CD and through the adjustment of the impedance measurements. C_{EIS} values are compared with those obtained at the lower currents used in this work, since C_{dl} is obtained from EIS measurements, in which it is determined the total interfacial area available. As can be seen, the tendency of both values match very well. The fact that the results are different is not strange, because the fitting procedure gives a value that represents the charge storage on the EDL and that obtained by CD features contributions from the electric double layer and faradaic charge transfer generated by surface groups of the carbons. Besides, the parameter L was not measured with a high precision.

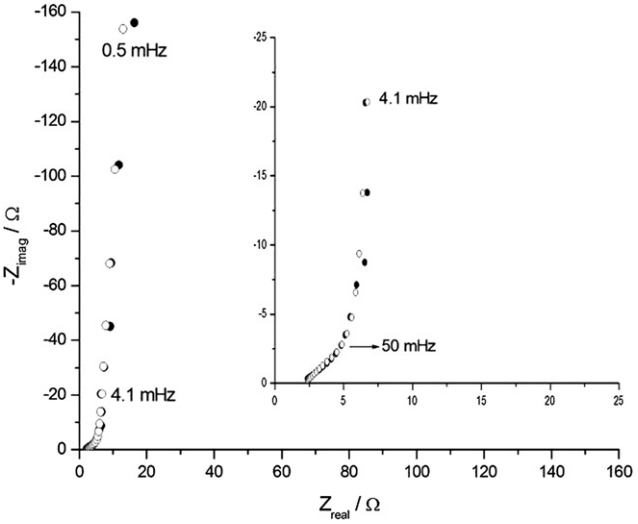

Fig. 6 – Experimental (●) and theoretical (○) spectra for M2 electrode. The insert shows the high-medium frequency range.

Table 2 – Capacity values obtained by CD and through the adjustment of the impedance measurements.

Muestra	C/Fg^{-1}	C_{EIS}/Fg^{-1}
M1	284	197
M2	230	174
M3	192	139
M4	180	133
S30	126	98

Commonly, charge densities in the double layer at plane electrodes are in the range of 1.6 10^{-5} to 5.10^{-5} Fcm^{-2} [1]. Assuming an average value of 3×10^{-5} Fcm^{-2} (C_{dl}^{0}), the interfacial area per electrode unit volume (a_i) for each electrode is obtained by means of the following equation,

$$C_{dl} = C_{dl}^{0} a_i \quad (6)$$

Table 3 contains the model parameters derived from the fitting procedure, corresponding to electrodes of different composition. The interfacial areas obtained from this method are quite similar for all the electrodes.

The electrochemically accessible carbon area, S_{EIE}, can be obtained after calculation of a_i,

$$S_{EIE} = \frac{a_i V}{m} \quad (7)$$

where V is the electrode volume and m is the total carbon mass. To find out the fraction of the total carbon area (sensed by N_2) that is accessible to the electrolyte, we define the accessibility parameter, A_c, as

$$A_c = S_{EIS}/S_{BET} \quad (8)$$

Table 3 exhibits the values of A_c obtained for each electrode. This parameter allows clarifying the differences in the capacities at low currents of each of the electrodes. The fact that C for M1 is higher than M2, the last with an interfacial area measured by BET significantly higher is because the electrolyte can access a much larger fraction of the porous matrix of M1 than to M2. While S30 has an area BET greater than the M3 and M4, the accessibility of the electrolyte to the porous matrix is much smaller, which leads to the fact that it is the carbon with lower C at low currents. In the same way can be explained the results for M3 and M4. While the latter has a significantly lower S_{BET}, the highest value of A_c generates similar capacities.

In addition, it must be pointed out the effective conductivity of the solid and of the electrolyte. Table 4 shows σ experimentally measured and σ_{EIS} and k_{EIS} determined with the adjustments of the impedance diagrams.

Table 3 – Values of A_c, S_{BET}, S_{EIS} and C_{dl} for all the electrodes.

Muestra	S_{BET}	C_{dl}	S_{EIS}	A_c	C
M1	1786	56	657	0.37	284
M2	2089	43	581	0.28	230
M3	1316	43	464	0.35	192
M4	995	45	422	0.42	180
S30	1664	35	345	0.21	126

Table 4 – Conductivity values obtained experimentally (σ) and from adjustment of impedance measurements (σ_{EIS} and k_{EIS}).

Muestra	$\sigma.10^2$	$\sigma_{EIS}.10^2$	$k_{EIE}.10^2$
M1	0.42	0.82	5.4
M2	0.66	1.7	5.4
M3	0.08	0.67	19.6
M4	0.09	0.52	1.3
S30	0.12	0.42	3.8

Results of solid conductivity values obtained by van der Pauw method and through EIS experiments show the same tendency. Because both, σ and κ, are expressed in Scm^{-1}, in order to make a direct comparison between the electrodes, σL and κL are the parameters that must be taken into account. Unluckily, the uncertainty on the measurement of the parameter L, make it impossible to analyze small differences between the electrode conductivities. On the other hand, these measurements allow concluding that in these materials, σ is the main responsible of the whole electrode resistivity, exhibiting in all electrodes less value than κ. However, for the electrode containing M4 and especially for that made of M2 is not possible to neglect any contribution to the total resistivity. As both of them have values of the same order, they contribute to the dynamic behavior of the electrode.

4. Conclusions

Carbon Xerogels with different pore size distribution were successfully obtained. Through basic electrochemical measurements, the dynamic behavior of every one electrode was evaluated. All xerogels, except for M3, showed higher capacities than the purchased carbon S30 for the currents employed in this work. Chronopotentiometry experiments performed at different discharge rates showed that M2 and S30 have similar behaviors; this fact allow concluding that the marked differences in C between these electrodes should be maintained using larger discharge currents. Electrochemical results show that through these carbons synthesis techniques it is possible to obtain very good materials to act as an SC.

Through a theoretical physicochemical model developed for porous electrodes, it was possible to obtain several parameters which permit to explain the different behavior of the electrodes. By comparing areas values obtained by BET method and from the EDL capacity obtained performing EIS experiments, the parameter A_c was proposed. It allows making a comparison of the electrolyte accessibility to the porous frame in each electrode, clearing up the differences in C at low currents.

Acknowledgments

This work was supported by: CONICET, Consejo Nacional de Investigaciones Científicas y Técnicas of Argentina, the Agencia Nacional de Promoción Científica y Tecnológica and the Universidad Nacional de La Plata. The financial support

received from the Government of Principado de Asturias PCTI (Ref. IB09-00201) and Ministerio de Ciencia e Innovación (Ref. MAT2008-00217/MAT) is also greatly acknowledged. E.G. Calvo also acknowledges a predoctoral research grant from FICYT.

REFERENCES

[1] Conway BE. Electrochemical supercapacitors. Scientific Fundamentals and Technological Applications. New York: Kluwer Academic/Plenum Publishers; 1999.
[2] Obreja VVN. On the performance of supercapacitors with electrodes based on carbon nanotubes and carbon activated material—A review. Physica E 2010;40:2596–605.
[3] http://www.panasonic.com/industrial/batteries-oem/oem/lithium-ion.aspx.
[4] Zubizarreta L, Arenillas A, Pis JJ, Pirard V, Job N. Studying chemical activation in carbon xerogels. J Mater Sci 2009;44:6583–90.
[5] Stoeckli F, Centeno TA. On the determination of surface areas in activated carbons. Carbon 2005;43:1184–90.
[6] Dubinin MM. Porous structure and adsorption properties of active carbons. In: WalkerJr PL, editor. Chemistry and physics of carbon, vol. 2. New York: Marcel Dekker; 1966. p. 51–120.
[7] Calvo EG, Juárez-Pérez EJ, Menéndez JA, Arenillas A. Fast microwave-assisted synthesis of tailored mesoporous carbon xerogels. J Colloid Interf Sci 2011;357:541–7.
[8] Dubinin MM. In: Danielli JF, Rosenberg MD, Cadenhead D, editors. Progress in surface and Membrane Science, vol. 9. New York: Academic Press; 1975.
[9] Stoeckli HF, Ballerini L. Evolution of Microporosity during activation of carbon. Fuel 1991;70:557–60.
[10] Parra JB, de Sousa JC, Bansal RC, Pis JJ, Pajares JA. Characterization of activated carbons by the BET equation-an alternative approach. Adsorpt Sci Technol 1995;12:51–66.
[11] van der Pauw J. A method of measuring specific resistivity and Hall effect of discs of arbitrary shape. Philips Res Repts 1958;13:1–9.
[12] Sing KSW. Reporting physisorption data for gas/solid systems with Special reference to the determination of surface area and porosity. Pure Appl Chem 1985;57:603–19.
[13] Rodríguez J, Elola D, Laria D. Confined Polar Mixtures within Cylindrical Nanocavities. J Phys Chem B 2010;114:7900–8.
[14] Fernández PS, Castro EB, Real SG, Martins ME. Electrochemical behaviour of single walled carbon nanotubes – Hydrogen storage and hydrogen evolution reaction. Int J Hydrogen Energy 2009;34:8115–26.
[15] de Levie R. On porous electrodes in electrolyte solutions. Electrochim Acta 1963;8:751–80.
[16] Castro EB, Real SG, Bonesi A, Visintin A, Triaca WE. Electrochemical impedance characterization of porous metal hydride electrodes. Electrochim Acta 2004;49:3879–90.
[17] Meyers JP, Doyle M, Darling RM, Newman JJ. The impedance response of a porous electrode composed of intercalation particles. J Electrochem Soc 2000;147:2930.
[18] Nelder JA, Mead R. A simplex method for function minimization. Comput J 1965;7:308–13.
[19] Visintin A, Castro EB, Real SG, Triaca WE, Wang C, Soriaga MP. Electrochemical activation and electrocatalytic enhancement of a hydride-forming metal alloy modified with palladium, platinum and nickel. Electrochim Acta 2006;51:3658–67.